Available online at www.sciencedirect.com

ScienceDirect

Nuclear Physics A 1005 (2021) 122017

NUCLEAR PHYSICS A

www.elsevier.com/locate/nuclphysa

XXVIIIth International Conference on Ultrarelativistic Nucleus-Nucleus Collisions (Quark Matter 2019)

Parton energy loss: new theoretical progress

Konrad Tywoniuk

Department of Physics and Technology, University of Bergen, 5007 Bergen, Norway

Abstract

The physics of jet quenching combines the dynamics of the QCD parton shower with bremsstrahlung radiation and decoherence processes induced by interactions with an underlying medium. Here we present a brief overview of the established features of medium-induced bremsstrahlung spectrum in a deconfined QCD plasma, highlight the aspect of rapid jet showering inside the medium and compute the resulting energy lost out of the jet cone in heavy-ion collisions.

Keywords: perturbative QCD, medium-induced bremsstrahlung, jet quenching

1. Introduction

Hard probes, such as high-p_T particles and jets, are produced abundantly in hadronic collisions at the LHC and RHIC. The concept of "jet quenching" is a generic placeholder to address modifications of such processes in heavy-ion collisions away from their proton-proton baseline [1, 2]. The theoretical description of parton propagation and branching in a deconfined nuclear medium has been developing over more than two decades, for recent reviews see [3, 4]. In addition to drag experienced by the partons due to elastic energy loss, the transverse momentum broadening plays an important role because it also opens the possibility for medium-induced bremsstrahlung. When performing a jet measurement with a specific cone size R the challenge is to predict how much of the original parton's energy remains inside that cone, and how much leaks out. The missing energy ultimately determines the shift of the underlying production spectrum and results in an overall suppression of the jet sample in a given p_T bin.

Let us first recall the basics of QCD radiation in vacuum (meaning in the absence of interactions). An initiating jet parton with energy p_T can radiate within a cone with opening angle R, corresponding to the radius of the experimentally reconstructed jet. In the soft and collinear limit, the spectrum of gluon emissions,

$$\mathrm{d}I \simeq \frac{2\alpha_s C_R}{\pi}\frac{\mathrm{d}z}{z}\frac{\mathrm{d}\theta}{\theta}\,, \tag{1}$$

https://doi.org/10.1016/j.nuclphysa.2020.122017
0375-9474/

where C_R is the color charge of the parent, is enhanced by a two logarithmic divergences for small values of the longitudinal momentum sharing fraction z and emission angle θ. Th phase space for *inter-jet* emissions, or the total probability of radiating inside a jet cone, is

$$\text{Prob} = \frac{\alpha_s C_R}{\pi} \log^2 \frac{p_T R}{Q_0} \,. \tag{2}$$

When this probability becomes large, i.e. Prob $> O(1)$, multiple emissions have to be accounted for. What drives the enhancement is the separation of the jet scale $p_T R$ and the non-perturbative cut-off $Q_0 \sim \Lambda_{\text{QCD}}$. Accounting for many such splittings is achieved through evolution equations that obey angular ordering as dictated by the coherence properties of multi-gluon emissions.

In addition, for small cone-size jets one should also resum potentially large logarithms in $1/R$. The distributions of micro-jets, with (small) cone size R, originating from a parton of species i, carrying a momentum fraction z of the total energy $f_{\text{jet}/i}(z,t)$, where $t = \log 1/R$, is similarly given by the evolution equation

$$\frac{\partial}{\partial \tilde{t}} f_{\text{jet}/i}(z,\tilde{t}) = \int_0^1 \frac{\mathrm{d}z'}{z'} \frac{\alpha_s}{\pi} P_{ji}(z') f_{\text{jet}/j}\left(\frac{z}{z'},\tilde{t}\right) , \tag{3}$$

where $P_{ji}(z)$ $(i = q, g)$ are the regularized Altarelli-Parisi splitting kernels [5, 6, 7]. This is equivalent to the celebrated DGLAP evolution equations.

From the point of view of medium interactions, it is a relevant question to ask whether some of these $O(1)$ emissions take place at early times, while the projectile is still inside the medium. In this context, the relevant quantity to consider is the formation time t_{f}. It can be estimated as the time when a dipole consisting of the products of the splitting, whose transverse size is grows linearly with time $x_\perp \sim \theta t$, can be resolved by a wave-length $\lambda_\perp \sim 1/k_\perp \sim 1/(\omega\theta)$. Demanding that $x_\perp \sim \lambda_\perp$ defines the formation time to be

$$t_{\text{f}} \sim \frac{1}{\omega\theta^2} \sim \frac{\omega}{k_\perp^2} \,. \tag{4}$$

The first equality indicates that, at fixed emission angle θ, soft gluons are created at late times. This is indeed what is expected from the conventional QCD cascade. Hard emissions, on the other hand, can occur at short t_{f}.

In the following, we will briefly recall the physics of parton propagation and branching in a dense medium. This allows us to compute the total amount of energy taken away from a single parton and the resulting shift of the underlying spectrum. We then turn to the question of jets and exploit the occurrence of hard QCD radiation early in the medium that act as new sources of bremsstrahlung and enhance energy loss. Opening up the jet cone sheds light on the delicate balance between allowing for more early, hard QCD radiation ("wider" jets) that lead to stronger energy loss and the recovery of soft fragments within the cone. This interplay ultimately is a probe of the degree of thermalization of the soft fragments within a medium-modified jet.

2. Medium-induced processes

A fast particle moving through a medium, will experience transverse momentum broadening, according to

$$\frac{\mathrm{d}\langle k_\perp^2 \rangle}{\mathrm{d}t} = \hat{q} \,, \tag{5}$$

where $\hat{q}$ is the jet transport coefficient that plays a role as a diffusion parameter. For a medium in thermal equilibrium, it scales as $\hat{q} \sim m_D^2/\ell_{\text{mfp}} \sim g^4 T^3$ (up to logarithms), where the Debye mass $m_D \sim gT$ represents a typical momentum scale of that is exchanged with the medium and the mean free path $\ell_{\text{mfp}} = (n\sigma_{\text{el}})^{-1} \sim m_D^2/(\alpha_s^2 n) \sim 1/(g^2 T)$, where $n \sim T^3$ is the density of scattering centers.

Heuristic discussion. Momentum broadening alters the trajectories of particles in the medium, but it also affects the possible radiation that occurs during the passage through the medium. In order to estimate the spectrum of such emissions, let us consider the formation time of gluons that are affected by this transverse momentum broadening, i.e. $t_{\rm f} \sim \omega/k_\perp^2$ where the magnitude of $k_\perp^2$ is governed by Eq. (5). We obtain that the typical formation or branching time scales as

$$t_{\rm f} \sim t_{\rm br} \sim \sqrt{\frac{\omega}{\hat{q}}}\,. \tag{6}$$

In turn, the typical transverse momentum acquired at emission time, is $k_\perp^2 \sim k_{\rm br}^2 = \sqrt{\omega\hat{q}}$. Instead of the double-logarithmic structure of vacuum radiation, the bremsstrahlung spectrum of medium-induced gluons can be written per unit time dt suggestively as

$$\mathrm{d}I = \frac{\alpha_s C_R}{\pi}\frac{\mathrm{d}\omega}{\omega}\frac{\mathrm{d}t}{t_{\rm br}}\,. \tag{7}$$

We note that the first two terms in the product, related to the combination of the running coupling constant and the color charge of the emitter as well as the soft divergence term dω/ω, resemble closely the structure of vacuum radiation.

While Eq. (7) was derived from purely heuristic arguments, it reproduces remarkably well the behavior of the full, analytical spectrum, to be reviewed in more detail below. Let us therefore describe three distinct regimes of the bremsstrahlung spectrum, that features two characteristic length scales of the medium.

Bethe-Heitler regime: We start with the regime where the branching time is of the order of the mean free path in the medium, i.e. $t_{\rm br} \sim \ell_{\rm mfp}$ or $\omega \sim \omega_{\rm BH} = \hat{q}\ell_{\rm mfp}^2 \sim T$. Our heuristic estimate gives that the spectrum of emissions after traversing a length L inside the medium is

$$\mathrm{d}I = \frac{\alpha_s C_R}{\pi}\frac{L}{\ell_{\rm mfp}}\frac{\mathrm{d}\omega}{\omega}\,. \tag{8}$$

This is the so-called Bethe-Heitler bremsstrahlung spectrum that describes emissions due to incoherent scattering off the medium that is proportional to the number of scatterers $N_{\rm scat} \sim L/\ell_{\rm mfp}$.

LPM regime: The other length scale in the game is indeed the extent of the medium L and when the number of scatterings $N_{\rm scat} = L/\ell_{\rm mfp} > 1$ one has to consider interference effects between different scattering centers. For branching times $\ell_{\rm mfp} < t_{\rm br} < L$, the spectrum is simply given by

$$\mathrm{d}I = \frac{\alpha_s C_R}{\pi}\sqrt{\frac{\hat{q}L^2}{\omega}}\frac{\mathrm{d}\omega}{\omega}\,. \tag{9}$$

The soft energy divergence is indeed stronger that in vacuum, i.e. $\omega^{-3/2}$, which is a consequence of the Landau-Pomeranchuk-Migdal (LPM) interference [8, 9, 10, 11]. The number of effective scattering centers is in this case $N_{\rm eff} = N_{\rm scat}/N_{\rm coh} \sim L/t_{\rm br}$, where the number of coherent scatterings per radiation is $N_{\rm coh} \sim t_{\rm br}/\ell_{\rm mfp}$.

From Eq. (9) we also identify the maximal energy due to medium rescattering $\omega_c = \hat{q}L^2$, which corresponds to long branching times $t_{\rm br} = L$. The transverse momentum accumulated is then simply $k_\perp^2 = \hat{q}L$. The fact that the spectrum in Eq. (9) scales linearly with L also indicates that the splitting can happen at any place in the medium with equal probability.

UV regime: Finally, when the gluon energy (transverse momentum) is large, i.e. $\omega > \omega_c$ ($k_\perp^2 > \hat{q}L$), the analysis is slightly more involved. The underlying $k_\perp$ spectrum for $k_\perp^2 \gg \hat{q}L$ is steeply

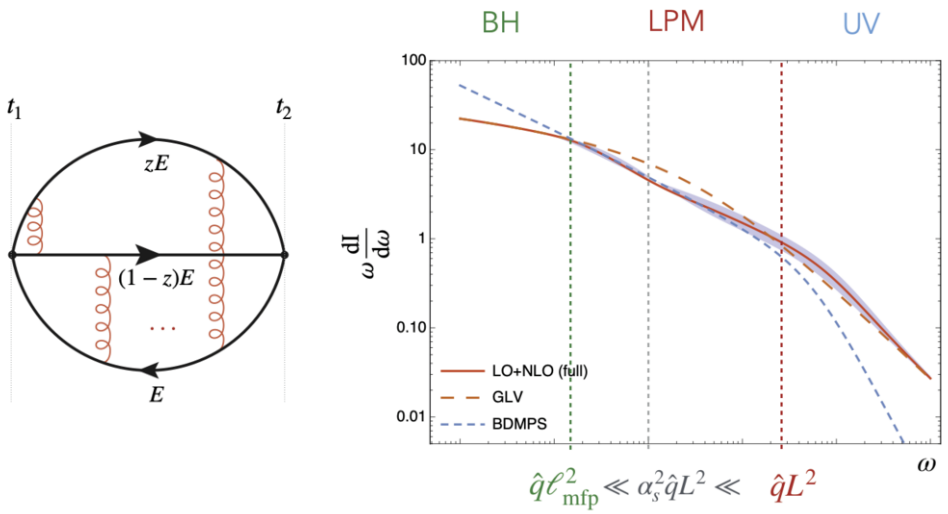

Fig. 1. (Left) Illustration of the three-point function that contributes to the spectrum of medium-induced gluons. (Right) Spectrum of medium-induced gluons $\omega \mathrm{d}I/\mathrm{d}\omega$ as a function of the gluon energy ω. Figure adapted from [13].

falling, i.e. $\sim 1/k_\perp^4$. Hence, the integral over $k_\perp^2$ is dominated by its lower limit. Since large formation times $t_\mathrm{f} > L$, or $k_\perp^2 < \omega/L$, are suppressed by the LPM effect, the range of available transverse momenta is bound from below by $k_\perp^2 > \omega/L > \hat{q}L$. The spectrum is again dominated by a single scattering, hence proportional to the length times the density of scattering centers $\alpha_s^2 nL \sim \hat{q}L$, and reads

$$\mathrm{d}I \sim \frac{\alpha_s C_R}{\pi} \hat{q} L \frac{\mathrm{d}\omega}{\omega} \int_{\omega/L}^{\infty} \frac{\mathrm{d}k_\perp^2}{k_\perp^4} = \frac{\alpha_s C_R}{\pi} \frac{\omega_c}{\omega} \frac{\mathrm{d}\omega}{\omega} \tag{10}$$

This corresponds to the high-energy regime of GLV spectrum [12]. The fact that the spectrum is again proportional to the number of scattering centers, suggests that this regime is again dominated by rare (incoherent) interactions with the medium.

Medium-induced radiation. The heuristic presentation of the spectrum of medium-induced gluons outlined above gives provides a quite accurate description compared to the full theoretical description. Consider the splitting of a parent parton a, carrying energy E, into two daughter partons b and c carrying energies zE and $(1-z)E$, respectively, see Fig. 1 (left). The spectrum of medium-induced splitting is given as

$$z \frac{\mathrm{d}I_{ba}}{\mathrm{d}z} = \frac{\alpha_s \, z p_{ba}(z)}{(z(1-z)E)^2} \, 2\mathrm{Re} \int_0^\infty \mathrm{d}t_2 \int_0^{t_2} \mathrm{d}t_1 \, \partial_{\boldsymbol{x}} \cdot \partial_{\boldsymbol{y}} \Big[(\boldsymbol{x}|\mathcal{K}_{ba}(t_2,t_1)|\boldsymbol{y}) - (\boldsymbol{x}|\mathcal{K}_{ba}^{(0)}(t_2,t_1)|\boldsymbol{y}) \Big]_{\boldsymbol{x}=\boldsymbol{y}=0} , \tag{11}$$

where $p_{ba}(z)$ are the unregularized Altarelli-Parisi splitting functions. The Green's function $\mathcal{K}(t_2,t_1)$ incorporates the effects of multiple scattering in the medium between an initial time t_1 and a final time t_2 of three propagators. This is illustrated in Fig. 1 (left), where the the two times correspond to the splitting time in the amplitude and complex conjugate amplitude, respectively. The upper and middle lines correspond to the daughter partons propagating after the splitting occurred at time t_1 in the amplitude, while the lower line corresponds to the parent before the splitting occurs at time t_2 in the complex conjugate amplitude. This can be generally written, in arbitrary representation,

in implicit form as

$$\mathcal{K}(t_2,t_1) = \mathcal{K}^{(0)}(t_2-t_1) + \int_{t_1}^{t_2} \mathrm{d}s\, \mathcal{K}^{(0)}(t_2-s) v(s) \mathcal{K}(s,t_1)\,, \tag{12}$$

where $v(s)$ represents the three-body potential. In Eq. (11) it is convenient to write the representation of the three-point function in transverse coordinate space which is in turn equivalent, through a Fourier transform, to the transverse momentum space representation.

The kernel $v(t)$ accounts for the exchange of momenta between all three propagating pieces of the correlator, see Fig. 1, at a given instant t during the propagation. In coordinate representation we write

$$v_{ba}(\boldsymbol{x},t) = \frac{C_b + C_c - C_a}{2}\,\tilde{v}(\boldsymbol{x},t) + \frac{C_c + C_a - C_b}{2}\,\tilde{v}(z\boldsymbol{x},t) + \frac{C_a + C_b - C_c}{2}\,\tilde{v}((1-z)\boldsymbol{x},t)\,, \tag{13}$$

where C_a, C_a and C_c are the color factors associated with partons in representations a, b and c, respectively. The elementary two-body potential, stripped of the color factor, reads

$$\tilde{v}(\boldsymbol{x},t) = \int_{\boldsymbol{q}} \frac{\mathrm{d}\sigma_{\mathrm{el}}}{\mathrm{d}^2\boldsymbol{q}} \left(1 - \mathrm{e}^{i\boldsymbol{q}\cdot\boldsymbol{x}}\right) \approx \frac{1}{4N_c}\boldsymbol{x}^2\hat{q}_0(t) \ln\frac{1}{\mu^2\boldsymbol{x}^2} + \ldots \tag{14}$$

where we only write explicitly the first dominant term of the expansion. We have also assumed an IR screening the perturbative $2 \to 2$ elastic scattering cross section $\mathrm{d}\sigma_{\mathrm{el}}/\mathrm{d}\boldsymbol{q}^2 \simeq g^4 n/q_\perp^4$ at scale $q_\perp \sim \mu$, which is related to the Debye screening mass. Finally, $\mathcal{K}^{(0)}_{ba}(\Delta t)$ is the three-point correlator in vacuum, and reads simply

$$(\boldsymbol{x}|\mathcal{K}^{(0)}_{ba}(t_2,t_1)|\boldsymbol{y}) = \delta_{ba}\,\frac{\omega}{2\pi i\,\Delta t}\exp\left\{i\frac{\omega}{2}\frac{(\boldsymbol{x}-\boldsymbol{y})^2}{\Delta t}\right\}, \tag{15}$$

where $\Delta t = t_2 - t_1$ and $\omega = z(1-z)E$. It is explicitly subtracted in Eq. (11) in order to remove all vacuum like contributions to the spectrum.

There exists at least three approaches to compute this correlator. First, one can attempt a brute-force order by order evaluation of the expansion in Eq. (12) which is usually referred to as the **opacity expansion** [12, 14].[1] While many calculations in the current literature are based on the first order in opacity ($N = 1$), recently there has been a lot of effort devoted to computing higher orders [17, 18, 19]. Second, by neglecting the logarithmic contribution and substituting the first order of Eq. (14) for the full potential, that is $\tilde{v}(\boldsymbol{x}) \propto \boldsymbol{x}^2\hat{q}$, one can solve the three-point correlator analytically. This typically goes under the name of the **harmonic oscillator approximation** (HO), see e.g. [20, 21]. A third way is to solve the evolution equation numerically, see originally [22] and [23, 24, 25] for recent work.

Finally, it was also recently suggested to shift the point of expansion in order to make the resummation more efficient [26, 13]. Concretely, in [13] it was suggested to explicitly extract the harmonic oscillator term, i.e.

$$\tilde{v}(\boldsymbol{x},t) = \tilde{v}_{\mathrm{HO}}(\boldsymbol{x},t) + \delta\tilde{v}(\boldsymbol{x},t)\,, \tag{16}$$

where $\tilde{v}_{\mathrm{HO}}(\boldsymbol{x},t) \propto \boldsymbol{x}^2\hat{q}\ln Q_{\mathrm{sub}}^2/\mu^2$ and Q_{sub} is a suitable matching scale. The advantage of this trick is that the 0th order (harmonic oscillator) solution is known analytically and higher-order corrections amount to small perturbations around it. It also naturally embodies the expected behavior in the IR and UV regimes.

The medium-induced spectrum in the soft limit $z \ll 1$ (or alternatively $E \to \infty$), where $\omega \simeq zE$, is plotted in Fig. 1 (right). We have explicitly marked the characteristic energy scales $\omega_{\mathrm{BH}} =$

[1] See also [15, 16] for related results in the higher-twist formalism.

$\hat{q}\ell^2_{mfp}$ and $\omega_c = \hat{q}L^2$ according to the discussion above. We have additionally plotted the results from the $N = 1$ (denoted by "GLV" in the figure) (orange, dashed curve) and HO (denoted by "BDMPS") approximations (blue, dotted curve). Finally, we also plot the results from considering the decomposition in Eq. (16) up to next-to-leading order [13] which provides a good description across the three distinct regimes.

Modification of spectra due to energy loss. In order to calculate the full amount of energy lost by a parton, we should account for multiple emissions. Assuming independent emissions that can easily be achieved leading to the definition of a probability distribution $\mathcal{P}(\epsilon; R, L)$ to lose energy ϵ out of cone with radius R during the in-medium propagation along L (we typically will suppress the cone size and length dependence when writing this distribution). It is then given by [27, 20]

$$\mathcal{P}(\epsilon) = \mathcal{P}_0\delta(\epsilon) + \sum_{n=1}^{\infty}\frac{1}{n!}\prod_{i=1}^{n}\int_0^\infty \mathrm{d}\omega_i \frac{\mathrm{d}I_>}{\mathrm{d}\omega_i}\mathcal{P}_0\ \delta\left(\epsilon - \sum_{i=1}^{n}\omega_i\right), \tag{17}$$

where $\mathcal{P}_0 = \exp\left(-\int_0^\infty \mathrm{d}\omega \frac{\mathrm{d}I_>}{\mathrm{d}\omega}\right)$ is the no-emission probability. In Laplace space, this lengthy expression simplifies to

$$\tilde{\mathcal{P}}(\nu) = \exp\left[\int_0^\infty \mathrm{d}\omega \frac{\mathrm{d}I_>}{\mathrm{d}\omega}\ (\mathrm{e}^{-\omega\nu} - 1)\right]. \tag{18}$$

The subscript ">" on the spectrum in the expressions above implies that we only consider gluons that are emitted a larger angles than the cone size. This can be calculated from the full double-differential spectrum but for our purposes it can easily be accounted for assuming that medium-induced quanta typically accumulate transverse momentum of the order of $\sim \sqrt{\hat{q}L}$.[2]

The latter representation is particularly useful, since the medium-modified spectrum,

$$\frac{\mathrm{d}\sigma_{\rm med}}{\mathrm{d}p_T} = \int_0^\infty \mathrm{d}\epsilon\, \mathcal{P}(\epsilon)\ \frac{\mathrm{d}\sigma_{\rm vac}}{\mathrm{d}p'_T}\bigg|_{p'_T = p_T+\epsilon} \approx \frac{\mathrm{d}\sigma_{\rm vac}}{\mathrm{d}p_T}\int_0^\infty \mathrm{d}\epsilon\, \mathcal{P}(\epsilon)\mathrm{e}^{-\epsilon\frac{n}{p_T}} = \frac{\mathrm{d}\sigma_{\rm vac}}{\mathrm{d}p_T}Q(p_T)\,,\,, \tag{19}$$

is proportional to the vacuum spectrum times a jet suppression factor $Q(p_T)$ which, up to corrections, is nothing else than the Laplace transform at $\nu = n/p_T$, where n is the index of the steeply falling spectrum. It turns out that quenching is large whenever the multiplicity of radiated gluons is large, namely at the scale $\alpha_s^2\hat{q}L^2$ which is denoted explicitly in Fig. 1 (right) [27]. At this scale, a refined description, which accounts for secondary branchings, is needed [28, 29].

We plot the quenching factor for a single quark or gluon in Fig. 2 left and right panel, respectively, in dashed lines. The different colors denote the angle above which the bremsstrahlung gluons have to be emitted. We observe that with larger angles, the quenching gets weaker because of the gradual recovery of energy deposited at finite angles away from the jet as we open the reconstruction cone.

3. Multi-parton energy loss and jet quenching

As explained above, radiation induced by the medium has a limited range in energy or transverse momentum. However, hard radiation, with correspondingly short formation time, can occur if the phase space of the jet permits it. Such splittings correspond to vacuum-like emissions inside the medium [30, 31] so long as $k_\perp^2 > \sqrt{\hat{q}\omega}$, or $t_{\rm f} < t_{\rm d}$. The decoherence time $t_{\rm d}$ is the time-scale when a medium wave-length resolves a formed dipole and reads $t_{\rm d} \sim (\hat{q}\theta^2)^{-1/3}$. Furthermore, in order for the splitting to be resolved by the medium we have to demand that $t_{\rm d} < L$ which implies that $\theta > \theta_c = (\hat{q}L^3)^{-1/2}$. In the opposite case, the splittings are too narrow to be resolved during the passage through the medium and can therefore be considered to happen outside of the medium.

[2] It is worth mentioning that in this formulation the energy is lost independently via different mechanisms, and can be accounted for as $\mathcal{P}(\epsilon) = \int \mathrm{d}\epsilon_1\mathrm{d}\epsilon_2\, \delta(\epsilon-\epsilon_1-\epsilon_2)\mathcal{P}_{\rm rad}(\epsilon_1)\mathcal{P}_{\rm el}(\epsilon_2)$ and the spectrum is suppressed by a product of quenching factors.

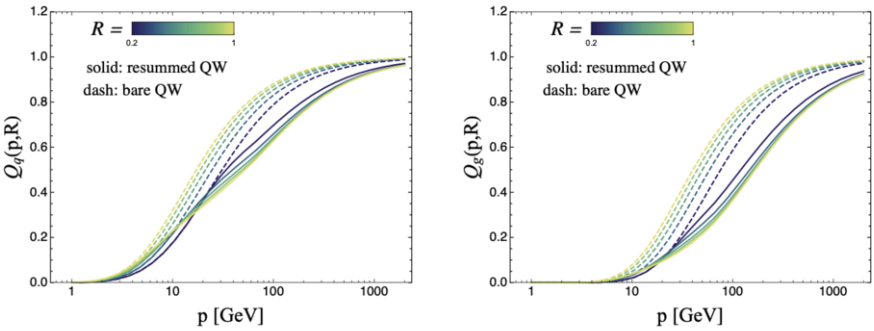

Fig. 2. The bare quenching factors and resulting collimators for quark (left) and gluon (right) initiated jets.

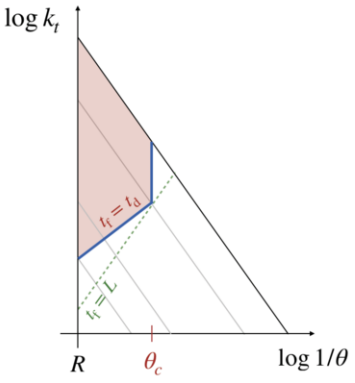

Fig. 3. Phase space illustrating hard, resolved jet emissions inside the medium.

These in-medium splittings have the following phase space

$$(\text{Prob.})_{\text{in}} = \bar{\alpha} \int_0^R \frac{\mathrm{d}\theta}{\theta} \int_0^{p_T} \frac{\mathrm{d}\omega}{\omega} \Theta_{\text{in}} = 2\bar{\alpha} \left(\ln \frac{p_T}{\omega_c} \ln \frac{R}{\theta_c} + \frac{2}{3} \ln^2 \frac{R}{\theta_c} \right), \tag{20}$$

where $\Theta_{\text{in}} \equiv \Theta(t_{\text{f}} < t_{\text{d}} < L)$. We obtain a potentially large logarithm of the jet energy, p_T, which indicates that the probability to form a vacuum cascade early inside the medium when $(\text{Prob.})_{\text{in}} > O(1)$, see also [32, 33]. This cascade fully retains its color coherence properties and is therefore ordered in angle.

At this stage we have clarified that a jet can branch several times before being affected by the medium, but we still have to understand how this color-coherent set of partons interact with the medium at later times. It turns out that, in the leading-logarithmic limit where $t_{\text{d}} \ll L$, all partons eventually get resolved inside the medium and lose energy independently [34]. For the medium-modified jet spectrum in Eq. (19), the single-parton quenching factor $Q(p_T)$ should be replaced by a multi-parton quenching factor $Q(p_T, R)$ that counts the number of hard in-medium jet splittings. This is achieved through a novel, non-linear evolution equation [30]

$$Q_a(p,R) = Q_a(p) + \int_0^R \frac{\mathrm{d}\theta}{\theta} \int_0^1 \mathrm{d}z \, \frac{\alpha_s}{\pi} p_{ba}(z) \, \Theta_{\text{in}} \left[Q_b(zp,\theta) Q_c((1-z)p,\theta) - Q_a(p,\theta) \right] . \tag{21}$$

where the evolving variable p is ultimately matched to p_T. At high-p_T, when the single parton quenching factor tends to unity $Q(p_T) \to 1$, the solution of the evolution is a fixed point at $Q(p_T, R) = 1$ as well.

We plot the fully resummed quenching factors for an initiating quark or gluon are plotted with full lines in Fig. 2. The curves show the interplay between opening up phase space for hard radiation at large angles, leading to enhanced energy loss, and the gradual recovering of energy, again at large angles.

4. Summary

To summarize, QCD jet showering depends on the possibility for copious soft and collinear radiation. These emissions are, up to leading-logarithmic accuracy, also endowed with a specific space-time structure of subsequent emissions. It is therefore reasonable to estimate that the hardest branches form very early, e.g. of the order of 0.1 fm for 100 GeV jets, thus making them especially sensitive to further medium interactions.

We have also briefly summarized the understanding of bremsstrahlung radiation in a deconfined QCD medium. It turns out that the emissions span a wide range of scales, from the Bethe-Heitler $\omega_{\rm BH} \sim T$ scale to $\omega_c \sim \hat{q}L^2$ (or $k_\perp^2 = \hat{q}L$). Harder emissions are suppressed in the medium and can therefore only arise as a results of jet showering. It turns out that in a dense medium, where $N_{\rm scat} \gg 1$, bremsstrahlung radiation constitute an efficient way of losing energy through the emission of multiple soft gluon with energies $\alpha_s^2\hat{q}L^2$ that get deflected and broadened up to large angles.

Finally, the total amount of energy lost by a jet is a superposition of quenching of all its emissions that were created, and subsequently resolved, early in the medium, i.e. with $t_{\rm f} < t_{\rm d}$ or $k_\perp^2 > \sqrt{\hat{q}\omega}$. This offers a new handle to measure the effect of $\hat{q}$. In particular, the R dependence of the jet spectrum is sensitive to the intricate balance between an increased phase space for hard radiation and the flow in and out of the jet cone that is closely related to the ability for soft, medium-induced jet fragments to thermalize with the underlying medium. The sensitivity of the details of phase space modeling is already built into many Monte Carlo models (such as MARTINI [35], the Saclay model [32] and the hybrid model [36]—the latter with a different phase space constraint), and therefore further theoretical studies are needed to understand this process in detail.

Acknowledgements. KT is supported by a Starting Grant from Trond Mohn Foundation (BFS2018-REK01) and the University of Bergen.

References

[1] D. d'Enterria, Landolt-Bornstein 23 (2010) 471. arXiv:0902.2011.
[2] A. Majumder, M. Van Leeuwen, Prog. Part. Nucl. Phys. 66 (2011) 41–92. arXiv:1002.2206.
[3] Y. Mehtar-Tani, J. G. Milhano, K. Tywoniuk, Int. J. Mod. Phys. A28 (2013) 1340013. arXiv:1302.2579.
[4] J.-P. Blaizot, Y. Mehtar-Tani, Int. J. Mod. Phys. E24 (11) (2015) 1530012. arXiv:1503.05958.
[5] M. Dasgupta, F. Dreyer, G. P. Salam, G. Soyez, JHEP 04 (2015) 039. arXiv:1411.5182.
[6] M. Dasgupta, F. A. Dreyer, G. P. Salam, G. Soyez, JHEP 06 (2016) 057. arXiv:1602.01110.
[7] Z.-B. Kang, F. Ringer, I. Vitev, Phys. Lett. B769 (2017) 242–248. arXiv:1701.05839.
[8] R. Baier, Y. L. Dokshitzer, A. H. Mueller, S. Peigne, D. Schiff, Nucl. Phys. B483 (1997) 291–320. arXiv:hep-ph/9607355.
[9] R. Baier, Y. L. Dokshitzer, A. H. Mueller, S. Peigne, D. Schiff, Nucl. Phys. B484 (1997) 265–282. arXiv:hep-ph/9608322.
[10] B. G. Zakharov, JETP Lett. 63 (1996) 952–957. arXiv:hep-ph/9607440.
[11] B. G. Zakharov, JETP Lett. 65 (1997) 615–620. arXiv:hep-ph/9704255.
[12] M. Gyulassy, P. Levai, I. Vitev, Nucl. Phys. B594 (2001) 371–419. arXiv:nucl-th/0006010.
[13] Y. Mehtar-Tani, K. TywoniukarXiv:1910.02032.
[14] U. A. Wiedemann, Nucl. Phys. B588 (2000) 303–344. arXiv:hep-ph/0005129.
[15] X.-N. Wang, X.-f. Guo, Nucl. Phys. A696 (2001) 788–832. arXiv:hep-ph/0102230.
[16] A. Majumder, Phys. Rev. D85 (2012) 014023. arXiv:0912.2987.
[17] G. Ovanesyan, I. Vitev, Phys. Lett. B706 (2012) 371–378. arXiv:1109.5619.
[18] M. D. Sievert, I. Vitev, Phys. Rev. D98 (9) (2018) 094010. arXiv:1807.03799.
[19] M. D. Sievert, I. Vitev, B. Yoon, Phys. Lett. B795 (2019) 502–510. arXiv:1903.06170.
[20] C. A. Salgado, U. A. Wiedemann, Phys. Rev. D68 (2003) 014008. arXiv:hep-ph/0302184.
[21] N. Armesto, C. A. Salgado, U. A. Wiedemann, Phys. Rev. D69 (2004) 114003. arXiv:hep-ph/0312106.
[22] S. Caron-Huot, C. Gale, Phys. Rev. C82 (2010) 064902. arXiv:1006.2379.
[23] X. Feal, R. Vazquez, Phys. Rev. D98 (7) (2018) 074029. arXiv:1811.01591.
[24] W. Ke, Y. Xu, S. A. Bass, Phys. Rev. C100 (6) (2019) 064911. arXiv:1810.08177.
[25] C. Andres, L. Apolinario, F. DominguezarXiv:2002.01517.
[26] Y. Mehtar-Tani, JHEP 07 (2019) 057. arXiv:1903.00506.
[27] R. Baier, Y. L. Dokshitzer, A. H. Mueller, D. Schiff, JHEP 09 (2001) 033. arXiv:hep-ph/0106347.
[28] J.-P. Blaizot, E. Iancu, Y. Mehtar-Tani, Phys. Rev. Lett. 111 (2013) 052001. arXiv:1301.6102.

[29] A. Kurkela, U. A. Wiedemann, Phys. Lett. B740 (2015) 172–178. arXiv:1407.0293.
[30] Y. Mehtar-Tani, K. Tywoniuk, Phys. Rev. D98 (5) (2018) 051501. arXiv:1707.07361.
[31] F. Domnguez, J. G. Milhano, C. A. Salgado, K. Tywoniuk, V. Vila, Eur. Phys. J. C80 (1) (2020) 11. arXiv:1907.03653.
[32] P. Caucal, E. Iancu, A. H. Mueller, G. Soyez, Phys. Rev. Lett. 120 (2018) 232001. arXiv:1801.09703.
[33] P. Caucal, E. Iancu, G. Soyez, JHEP 10 (2019) 273. arXiv:1907.04866.
[34] Y. Mehtar-Tani, K. Tywoniuk, Nucl. Phys. A979 (2018) 165–203. arXiv:1706.06047.
[35] B. Schenke, C. Gale, S. Jeon, Phys. Rev. C 80 (2009) 054913. arXiv:0909.2037.
[36] J. Casalderrey-Solana, D. C. Gulhan, J. G. Milhano, D. Pablos, K. Rajagopal, JHEP 10 (2014) 019, [Erratum: JHEP 09, 175 (2015)]. arXiv:1405.3864.